

 Open access • Journal Article • DOI:10.1063/1.324701

Microstructure and magnetic properties of Fe-Cr-Co-V alloys — Source link





Y. Belli, Masuo Okada, G. Thomas, M. Homma ...+1 more authors

Published on: 01 Mar 1978 - Journal of Applied Physics (American Institute of Physics)

Topics: Magnetic shape-memory alloy, Magnetic domain, Magnetic force microscope, Magnetic susceptibility and Thermomagnetic convection

Related papers:

- [Microstructure and magnetic properties of Fe-Cr-Co alloys](#)
- [Origin of coercivity in a Cr-Co-Fe alloy \(chromindur\)](#)
- [Fe-Cr-Co permanent magnet alloys containing Nb and Al](#)
- [Further studies of the miscibility gap in an Fe-Cr-Co permanent magnet system](#)
- [New ductile Cr-Co-Fe permanent magnet alloys for telephone receiver applications](#)

Share this paper:    

View more about this paper here: <https://typeset.io/papers/microstructure-and-magnetic-properties-of-fe-cr-co-v-alloys-1biej2h9qy>

Lawrence Berkeley National Laboratory

Lawrence Berkeley National Laboratory

Title

MICROSTRUCTURE AND MAGNETIC PROPERTIES OF Fe-Cr-Co-V ALLOYS

Permalink

<https://escholarship.org/uc/item/3td6m2fj>

Author

Belli, Y.

Publication Date

1977-12-01

MICROSTRUCTURE AND MAGNETIC PROPERTIES

OF Fe-Cr-Co-V ALLOYS

Y. Belli, M. Okada, G. Thomas

Department of Materials Science and Mineral Engineering
Materials and Molecular Research Division
Lawrence Berkeley Laboratory
University of California
Berkeley, California 94720

M. Homma and H. Kaneko

Department of Materials Science
Faculty of Engineering,
Tohoku University, Sendai, Japan 980.

NOTICE
This report was prepared as an account of work sponsored by the United States Government. Neither the United States nor the United States Department of Energy, nor any of their employees, nor any of their contractors, subcontractors, or their employees, makes any warranty, express or implied, or assumes any legal liability or responsibility for the accuracy, completeness or usefulness of any information, apparatus, product or process disclosed, or represents that its use would not infringe privately owned rights.

MICROSTRUCTURE AND MAGNETIC PROPERTIES

OF Fe-Cr-Co-V ALLOYS

Y. Belli, M. Okada, G. Thomas

Department of Materials Science and Mineral Engineering
Materials and Molecular Research Division
Lawrence Berkeley Laboratory
University of California
Berkeley, California 94720

M. Homma and H. Kaneko

Department of Materials Science
Faculty of Engineering,
Tohoku University, Sendai, Japan 980.

ABSTRACT

The relationship between the microstructure and magnetic properties of heat treated Fe-23wt%Cr-15wt%Co-5wt%V has been studied by transmission electron microscopy and Lorentz microscopy. Three different heat-treatments were adopted for the present investigations viz., 1) isothermal aging, 2) TMT (thermomagnetic treatment) + step-aging, 3) continuous cooling. It has been found that the magnetic properties of the alloy are very sensitive to the temperature of the thermomagnetic treatment. Step-aging gave the best magnetic properties, producing an elongated ferromagnetic phase, 300Å in diameter and 1200Å in length. Lorentz microscopy revealed domain walls and these lie within the Cr-rich phase and pinned by the Fe-rich phase in the isothermally aged alloy at 650°C. Magnetic domains of optimally step-aged alloy, 0.5µm in width, are elongated along

the direction of the applied magnetic field. The results suggest that the magnetic anisotropy is introduced parallel to the direction of the applied magnetic field during TMT and step-aging treatments.

INTRODUCTION

Fe-Cr-Co-V alloys are potential ductile permanent magnets with properties comparable to those of Alnico 5, which can be easily heat treated to produce optimum properties.⁽¹⁾ Previous work has concentrated on the base ternary Fe-Cr-Co alloy in which the microstructures and phase relationships are well characterized.^(2,3) The present investigation describes the microstructural changes of an Fe-23wt%Cr-15wt%Co-5wt%V alloy with various heat treatments (isothermal aging, thermomagnetic treatment, step-aging and continuous cooling) using electron microscopy. Since magnetic hardening of the alloy occurs on a very fine scale,⁽³⁾ transmission Lorentz electron microscopy has been used to study the magnetic domain structures, in an attempt to understand the magnetization reversal process of the alloy.

EXPERIMENTAL PROCEDURES

An Fe-23wt%Cr-15wt%Co-5wt%V alloy was homogenized at 1000°C for 1 hour in an argon atmosphere and quenched in ice water. The specimens were given various heat-treatments, and the magnetic properties of the specimen were measured with an automatic flux meter. Specimens for electron microscopy were thinned in an automatic jet polisher using an electrolytic solution of 23% perchloric acid and 77% acetic acid. Magnetic domain walls and domain configuration of the specimens were observed by the out-of-focus and displaced aperture methods.^(4,5)

RESULTS AND DISCUSSION

A. Microstructure

(1) Isothermal aging. The bright field micrographs (B.F.) shown in Fig. 1 are taken from the alloy aged for 1 hour at 660°C, 650°C, 640°C and 630°C, respectively. The phase with bright contrast is the Fe-rich phase (α_1) and the one with dark contrast is the Cr-rich phase (α_2).⁽³⁾ These micrographs suggest that the morphology of the microstructure and the volume fractions of the two phases are very sensitive to the aging temperature, i.e., the lower the aging temperatures, the finer the α_1 phase. The α_1 phase appears as rod shaped particles which become interconnected after aging at 640°C. These results are important in understanding the effect of thermomagnetic treatment (TMT) of the alloy at these temperatures.

(2) Thermomagnetic treatment and step-aging. It is reported that thermomagnetic treatment and step-aging have a beneficial effect on improving the magnetic properties of the system.^(1,3,6) Four different temperatures of thermomagnetic treatment (TMT) were chosen to investigate the effect of the TMT temperature on the magnetic properties and their microstructures. After TMT in a magnetic field of 2 KOe, the alloy was step-aged at 620°C, 600°C, 580°C, 560°C for 1 hour and subsequently aged at 540°C for 5 hours.

Fig. 2 illustrates the B.F. micrographs of the step-aged alloy after different TMT at (a) 660°C ($H_C \sim 420$ Oe), (b) 650°C ($H_C \sim 520$ Oe), (c) 640°C ($H_C \sim 370$ Oe) and (d) 630°C ($H_C \sim 80$ Oe), respectively. The coercive force of the alloy is remarkably affected by the temperature of the TMT. For example, Fig. 2(a) shows two morphologies of the α_1 phase viz., elongated α_1 particles, 300Å in diameter, and spherical α_1 particles, 135Å in diameter. Since the larger α_1 particles are elongated, they should

be formed during TMT, whilst the small α_1 must be nucleated after TMT. These morphologies are produced when the step-aging interval (ΔT) between $T_{\text{step } n} - T_{\text{step } (n-1)}$ is large.⁽³⁾ Fig. 2(b) corresponding to the optimum properties shows the α_1 phase, approximately 300Å in diameter and 1200Å in length, giving an aspect ratio of 4. In Fig. 2(c) and 2(d), the rod diameter is about 200Å and 140Å, and the length about 400Å and 220Å respectively. The fine spherical particles are absent in Fig. 2(c) and (d). This is believed to be due to the fact that the step-aging interval is small.

It is concluded that the morphology of microstructure and the shape or size of the ferromagnetic phase is very sensitive to the TMT temperature, resulting in different magnetic properties. This emphasizes that careful temperature control is needed to produce good magnetic properties.

(3) Continuous cooling. The step-aging process can be facilitated by continuous cooling, giving optimum magnetic properties.⁽¹⁾ In order to study the effect of continuous cooling rate on the magnetic properties and their microstructures, the alloy was thermomagnetically treated at 650°C for 1 hr since 650°C is the best temperature for TMT, and then continuously cooled to 540°C.

Fig. 3 shows the micrographs of the alloys continuously-cooled at the rate of (a) 1°C/min (Hc=220 Oe) and of (b) 0.25°C/min (Hc=520 Oe). These micrographs suggest that the morphology of the microstructure appears to be very similar, almost independently of the cooling rate. Since both specimens have the same TMT, the morphology of the microstructure must be established during TMT. This observation is similar to those observed in Alnico alloys.⁽⁷⁾

The coercive force of the fast cooled (1°C/min) specimens can be remarkably increased from 220 Oe to 520 Oe by isothermal aging at 540°C

for 14.5 hours after continuous cooling. But the coercive force of optimally cooled specimen (0.25°C/min) increases from 520 Oe to only 590 Oe by the same treatment. It has been observed that there is no noticeable difference in morphology of the microstructures between continuously cooled and low temperature aged alloys after continuous cooling. These results imply that the composition of the two phases differs depending on the continuous cooling rate, giving different coercive forces.

Therefore, there are two alternative methods to produce the optimum properties in this alloy. One is by continuous cooling at a rate of 0.25°C/min. The other is by cooling at a rate of 1°C/min and subsequently aging at low temperatures for long times.

B. Domain Structures

Fig. 4 shows the domain wall of the isothermally aged alloy at 650°C for 1 hr, imaged by the defocus method. The domain walls appear to be straight. From this micrograph it is uncertain where the domain wall exactly lies. To solve these uncertainties, the alloy was further aged at 650°C for 50 hrs, growing the α_1 particle from 150Å (in Fig. 4) to 900Å in diameter.

Fig. 5 shows the Fresnel micrographs of the over-aged alloy. The domain wall with black contrast (divergent wall) lies within the α_2 matrix phase. This stems from the fact that the domain wall energy of the α_2 phase is lower than that of the α_1 phase. After photographing Fig. 5(a), the specimen was taken out from the microscope and was put in a magnetic field. Then it was observed that the domain wall changed its position before (Fig. 5(a)), and after (Fig. 5(b)), applying the magnetic field. In Fig. 5(b), the domain wall exists in the α_2 phase and is slightly bent around the α_1 particles. These figures substantiate

that domain walls are pinned by the α_1 phase. It is concluded that the magnetization process of the isothermally aged alloy is due to domain wall pinning. Thus the coercive force would be given by the difference in wall energy of the two phases; $H_c \propto (W_{\alpha_1} - W_{\alpha_2})$ where W_{α_1} is the wall energy of the α_1 phase and W_{α_2} that of the α_2 phase. This mechanism has also been proposed for $\text{Sm}(\text{Co}, \text{Cu}, \text{Fe})_7$ magnets(8)

Fig. 6(a) and 6(b) are the Fresnel micrographs of the optimally step-aged alloy, showing a domain wall, and Fig. 6(c) and 6(d) are the Foucault micrographs (displaced aperture method). The observed domain wall is not straight. The domains are approximately $0.5\mu\text{m}$ wide, elongated along the direction of the applied magnetic field, and their size is smaller than that of the isothermally-aged alloy. The Foucault micrograph with higher magnification, as shown in Fig. 7 illustrates these features more clearly. The domain with black contrast is almost 1500\AA wide and is elongated in the direction of the applied magnetic field (the direction in which the α_1 phase is elongated). These observations suggest that the magnetic anisotropy is introduced parallel to the direction of the applied magnetic field after TMT and step-aging. Since the contrast mechanism of the magnetically inhomogeneous material (α_1 and α_2 phase) in Lorentz microscopy is complex, more experiments are needed to interpret the nature of the imaged domain walls in detail.

ACKNOWLEDGEMENTS

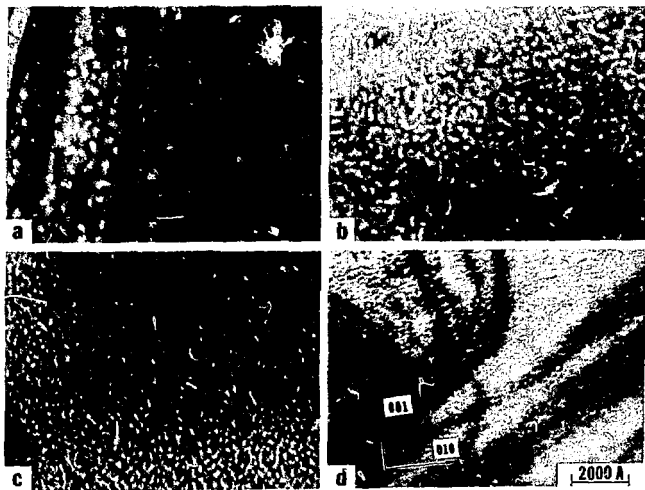
This research is sponsored by the United States Research Development Administration through the Lawrence Berkeley Laboratory

REFERENCES

1. H. Kaneko, M. Homma and T. Minowa, "Effects of V and V + Ti Additions on the Structure and Properties of Fe-Cr-Co Ductile Magnets", IEEE Trans. Magnetics, Mag-12, 177 (1976).
2. H. Kaneko, M. Homma, K. Nakamura, M. Okada, G. Thomas, "Phase Diagram of Fe-Cr-Co Permanent Magnet System", IEEE Trans. Magnetics, Mag-13, 1325 (1977).
3. M. Okada, G. Thomas, H. Kaneko, M. Homma, "Magnetic Properties and Microstructures of Fe-Cr-Co Alloys", to be published.
4. P.B. Hirsch, et al., "Electron Microscopy of Thin Crystals", Chap. 16, Butterworths, London, 1965.
5. J. P. Jakubovics, "Lorentz Microscopy and Application (TEM and SEM)", Electron Microscopy in Materials Science, Part IV, Commission of the European Communities, 1975.
6. H. Kaneko, M. Homma, K. Nakamura, "New Ductile Permanent Magnet of Fe-Cr-Co System", AIP Conf. Proc., No. 5, 1088 (1971).
7. K. J. De Vos, "Alnico Permanent Magnet Materials", Vol. 1, Magnetism and Metallurgy, 473 (Academic Press, 1969).
8. J. D. Livingston and D. L. Martin, "Microstructure of Aged (Co, Cu, Fe)₇Sm Magnets", J. of Appl. Phys., 48, 1350 (1977).

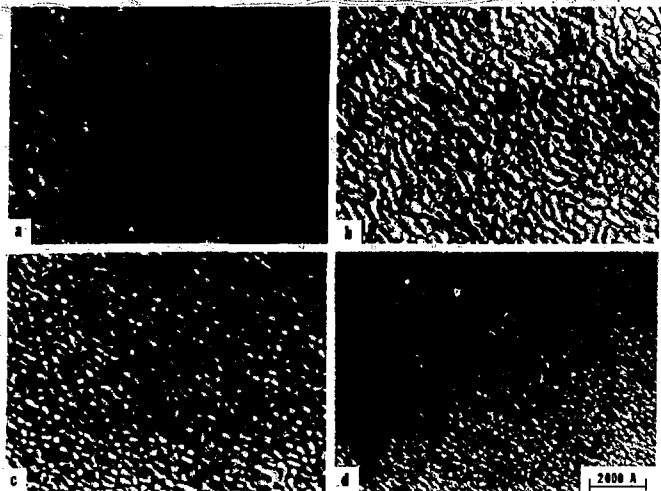
FIGURE CAPTIONS

- Fig. 1. Bright Field (B.F.) micrographs taken from the isothermally aged alloy for 1 hr at (a) 660°C, (b) 650°C, (c) 640°C and (d) 630°C.
- Fig. 2. B.F. micrographs taken from the step-aged alloy after thermomagnetic treatment for 1 hr at (a) 660°C ($H_C \sim 420$ Oe), (b) 650°C ($H_C \sim 520$ Oe), (c) 640°C ($H_C \sim 370$ Oe) and (d) 630°C ($H_C \sim 80$ Oe).
- Fig. 3. B.F. micrographs taken from the continuous cooled alloys after TMT at 650°C for 1 hr at a rate of (a) 1°C/min ($H_C \sim 220$ Oe) and (b) 0.25°C/min ($H_C \sim 520$ Oe).
- Fig. 4. Fresnel micrographs taken from the alloy aged at 650°C for 1 hr.
- Fig. 5. Fresnel micrographs taken from the alloy aged at 650°C for 50 hrs, showing the domain wall is pinned by the α_1 particle.
- Fig. 6. Fresnel [(a), (b)] and Foucault micrographs [(c), (d)] of the step-aged alloy after TMT at 650°C for 1 hr ($H_C \sim 520$ Oe).
- Fig. 7. Foucault micrographs of the step-aged alloy after TMT at 650°C for 1 hr.



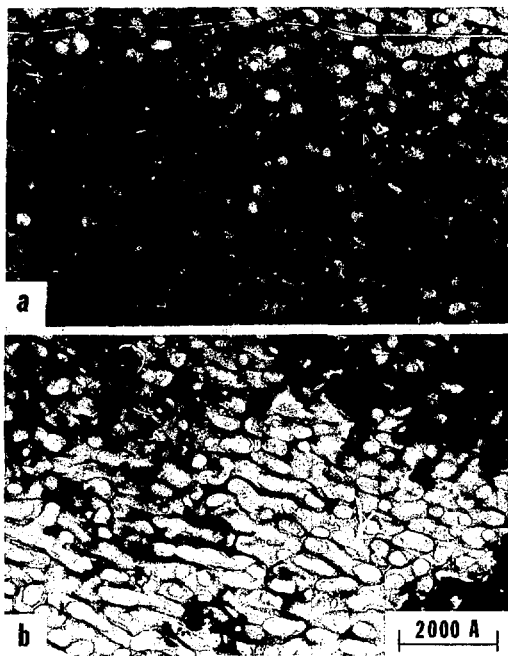
XBB 770-10356

Fig. 1



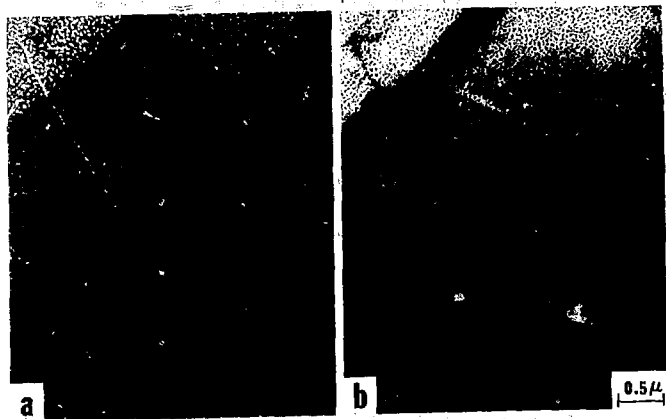
XBB 779-9128

Fig. 2



XBB 779-9130

Fig. 3



XBB 779-9125A

Fig. 4

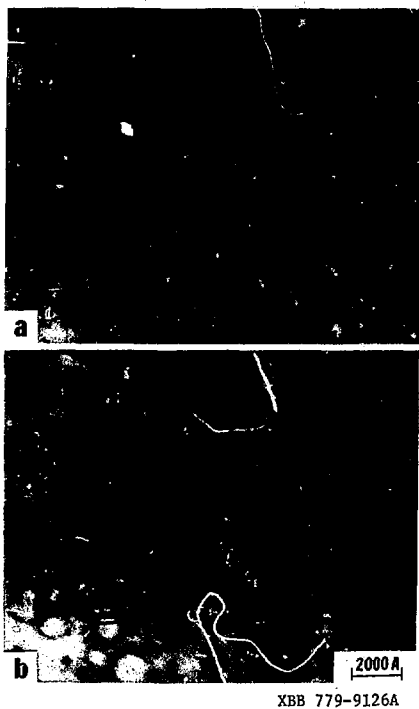
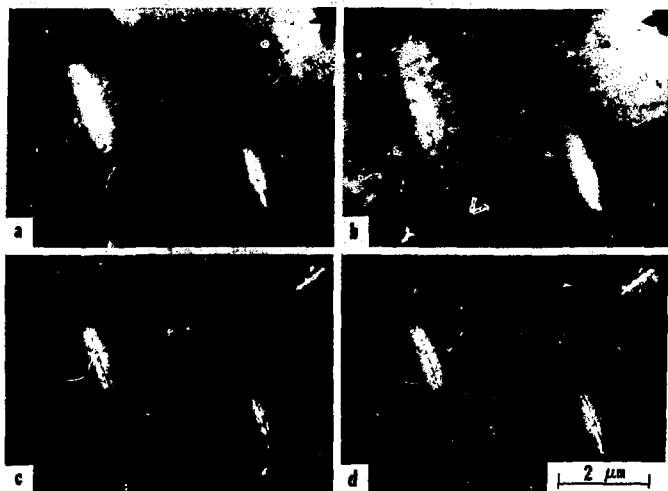
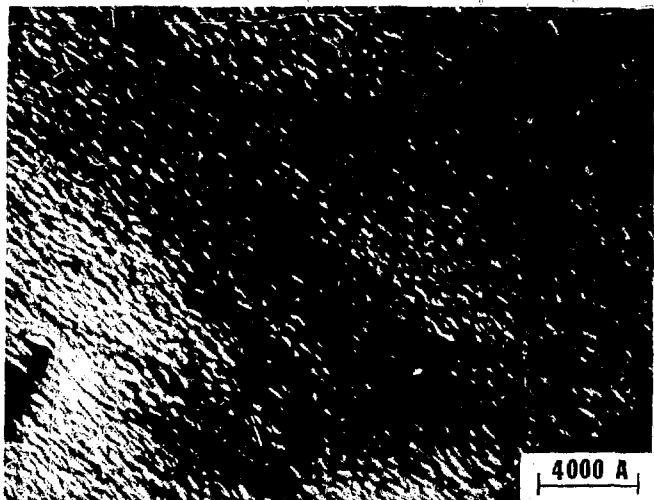


Fig. 5



XBB 779-9129

Fig. 6



XBB 779-9127

Fig. 7